HERSCHEL / PLANCK

HERSCHEL
Magnetic field of the solar generator

Rédigé par/*Written by*	**Responsabilité-Service-Société** ***Responsibility-Office -Company***	**Date**	**Signature**
A.LUC	EMC engineer	08/03/06	
Vérifié par/*Verified by*			
P.COUZIN	Electrical Interface Manager	13/03/06	
Approbation/*Approved*			
P.RIDEAU	Technical Manager	23/03/06	
J.J. JUILLET	Project manager	31.03.06	

Entité Emettrice : Alcatel Alenia Space - France
(détentrice de l'original)

HERSCHEL/PLANCK	DISTRIBUTION RECORD

DOCUMENT NUMBER : H-P-2-ASP-TN-1093

Issue : 1
Date: 08/02/2006

EXTERNAL DISTRIBUTION		INTERNAL DISTRIBUTION	
ESA	X	HP team	X
ASTRIUM	X		
ALCATEL ALENIA SPACE -Italia			
CONTRAVES			
TICRA			
TECNOLOGICA			
		Clt Documentation	Orig.

ENREGISTREMENT DES EVOLUTIONS / CHANGE RECORDS

ISSUE	DATE	§ : DESCRIPTION DES EVOLUTIONS § : CHANGE RECORD	REDACTEUR AUTHOR
1	08/02/2006	First issue	LUC A.

TABLE OF CONTENTS

1. INTRODUCTION

The aim of this technical note is to provide an evaluation of the magnetic field generated by the Herschel solar array on PACS cryo-harness.

2. REFERENCE DOCUMENT

[RD 01] : Herschel – Electrical Power Analysis and Design Report , HP-2-GAMI-AN-0014
[RD 02] : Planck Solar Array FM Data Pack, HP-4-GAMI-DP-0004 Rev B
[RD 03] : Magnetic moment analysis, HP-4-GAMI-AN-0016
[RD 04] : EMC Specification, H-P-1-ASPI-SP-0037

3. MAGNETIC FIELD ANALYSIS

3.1 Solar array mechanical layout

The Herschel mechanical design is presented in annex 1.

The layout of the panels is as follows:

Figure 1—1 : tern of reference axes

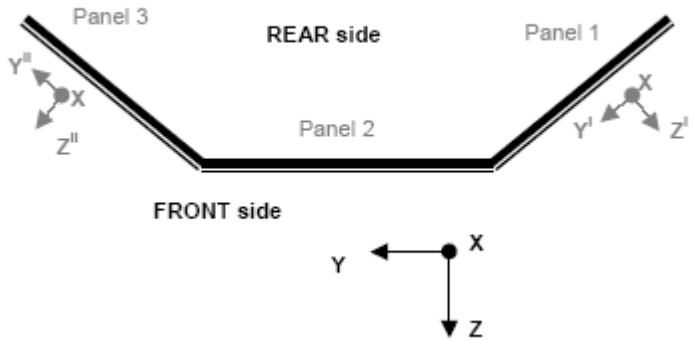

3.2 Electrical design of the solar array

The following table gives the magnetic moment (calculated by GA, see [RD 03]) of each section in the associated Z direction, i.e. roughly in the direction of the cryo-harness cables.

Section (ASED)	Section (Galileo Avionica)	Magnetic moment (A.m²)	Section in switching mode	Panel (Galileo Avionica)
30	1	-0.115		
29	2	0.049		
28	3	0.117		
27	7	0.099		
26	5	-0.066		
25	9	-0.055		
24	4	-0.072		
23	17	-0.015		
22	6	0. 118		
21	10	-0.198		
20	14	0.028		
19	18	0.063		
18	13	-0.522		
17	11	0.011		
16	15	0.082		
15	16	-0.027		
14	8	-0.048		
13	12	0.053		
12	19	-0.129		
11	29	0.004		
10	21	0.077		
9	22	-0.131		
8	26	0.11		
7	30	0.133	X	3
6	25	-0.34	X	1
5	23	-0.024	X	2
4	27	0.042	X	3
3	28	-0.034	X	1
2	20	-0.018	X	2
1	24	0.038	X	3

The minimum distances of the cryo-harness with regard to the 3 panels are :

	Distance (m)
Panel 1	0.87
Panel 2	0.83
Panel 3	0.35

Only one section is working and consequently generating a non constant magnetic field.
Remark : The magnetic moment calculated before correspond to variation of the current associated to the section between 0 and Imax. This approach is wrong with the S3R principle since the current is varying between Imax (short circuit) and I at operating point.

3.3 Power supply regulation principle

The solar array power is dumped by serial shunt regulators. A solar array section is periodically short circuited in the shunt regulator MOSFET. The periodical signal is pulse width modulated in order to vary the dumped average power. Nominally one shunt is working while the other are fully open or closed.

The current ripple towards the users power bus is filtered by the PCDU capacitor.

3.3.1 Variation of the current between operating point and short circuit

A solar cell acts as a current source with a non linear impedance characteristic.

The parameters issued of the I(V) curve are given in the following table for a section (worst case corresponding to End Of Life and Winter Solstice 0°, see [RD 01]) :

	At short circuit EOL WS 0°	At operating point EOL WS 0°	At open circuit
I (A)	2.06	1.68	0
U (V)	0	30	36.05

The solar cell working point is always below the maximum power point since the solar array voltage is regulated to 40V by shunts. At EOL the solar section generates this voltage with a current of 1.68 A. The short circuit current being 2.06 A, then the maximum current variation is $\Delta I = 0.38$ A

3.3.2 Transients

An evaluation of the current transients in the solar array due to the commutation of the S3R has been performed. Measurements and simulations have been performed. Results are presented in annex 2.

Main steps are explained here after :

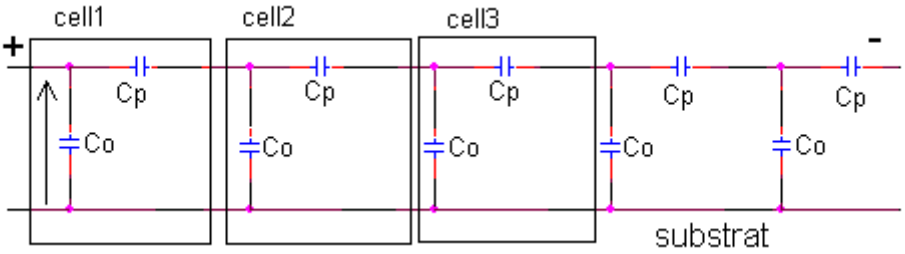

Figure 2.3.2-1 Solar Array string model

The transients exist either at the opening or at the closing of the shunt :

- At the opening of the shunt, the parasitic capacitances (Cp and C0) need to be recharged from 0 to 40V . All the current delivered by the solar array cells is consumed by these capacitances, increasing slowly the solar array panel voltage. A weak resonance generates an over current and a voltage transient.

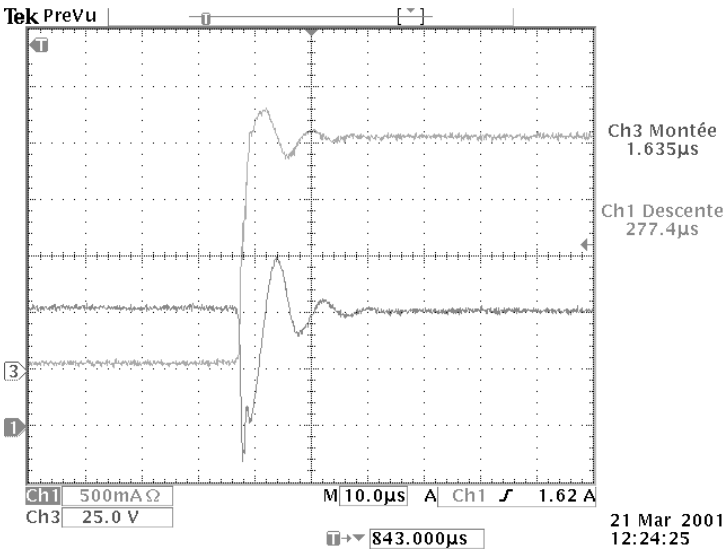

Ch1 : string current (500mA/div)
Ch3 : string voltage (25V/div)

- At the closing of the shunt, the parasitic capacitances discharge through the harness producing a current and voltage oscillations.

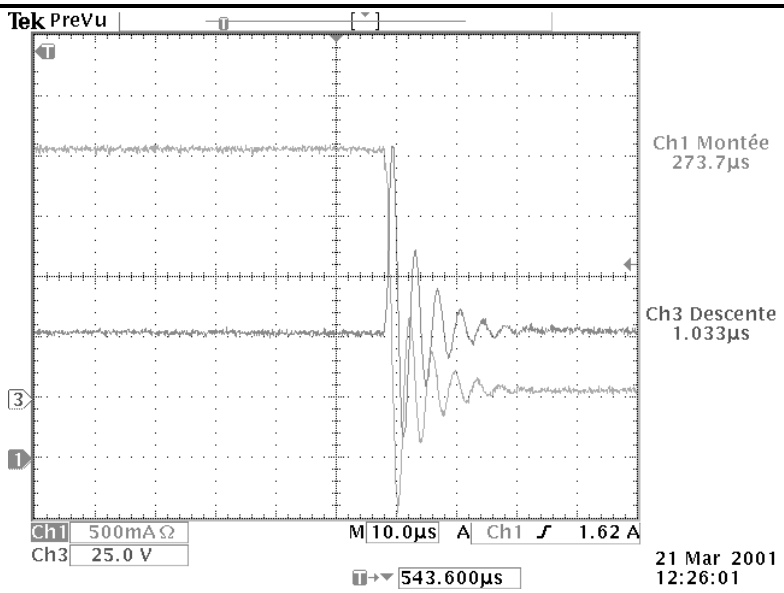

Ch1 : string current (500mA/div)
Ch3 : string voltage (25V/div)

Free wheel diode suppresses the oscillations at shunt closure.

Fourier transform performed on the last simulated signal gives the following spectrum (20 samples of the transients have been taken into account):
The results show that the signal is contained between the switching frequency and 150 kHz.

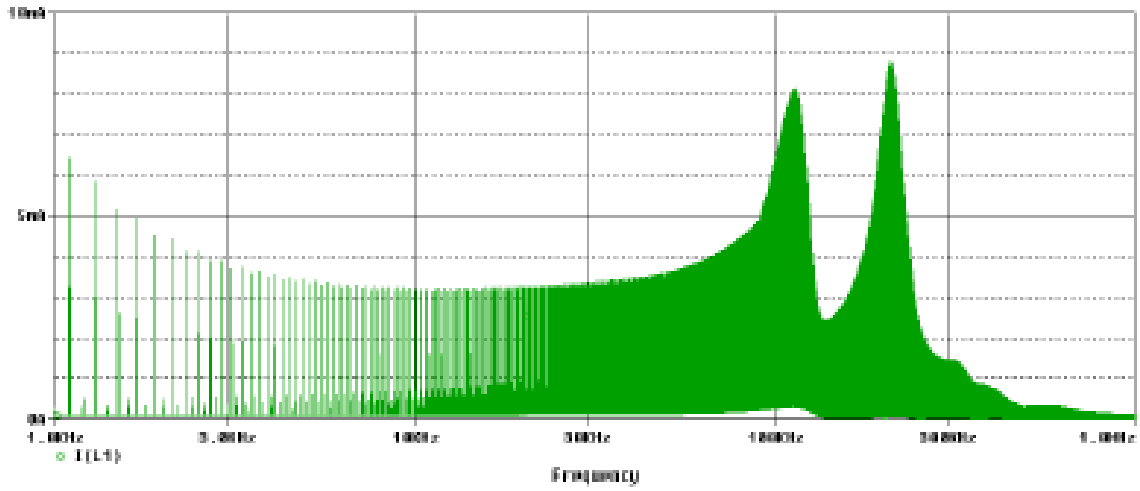

3.4 Magnetic field evaluation

Different points (A,B,C,D,E,F) of the cryo-harness are considered. Following table gives the position of these points and of the centre of the solar array section which can be in switching mode.

	X (m)	Y (m)	Z (m)
Center of section 28	0.459	-1.63	1.184
Center of section 25	0.459	-1.316	1.418
Center of section 23	0.491	0.153	1.845
Center of section 20	0.491	0.47	1.845
Center of section 24	0.459	0.98	1.681
Center of section 27	0.459	1.316	1.418
Center of section 30	0.459	1.63	1.184
Point A	0.687	-0.336	0.95
Point B	0.687	0	1.009
Point C	0.687	0.336	0.95
Point D	0.353	0.588	0.862
Point E	0.044	0.808	0.936
Point F	0.044	1.205	1.126

Worst cases which are considered are the following :

- Section 25, the worst case with regard to the magnetic moment and the nearest point of the cryo-harness which is point A.
- Section 30 which is the nearest section with regard to the cryo-harness point F

Evaluation of the field produced by a loop :

B is the magnetic field which is equal to the sum of two field components Bx and Br

Bx is the magnetic field component on the coil axis and Br the component in the radial direction

I is the current in the wire

R is the radius of the current loop

D_1 is the distance on axis from the center of the current loop to the point which is considered

D_2 is the radial distance from the axis of the current loop to the point which is considered

$$Bx = (I*\mu_0)/(2*\Pi*R)*1/(sqrQ)\ [E(k)*(1-\alpha^2-\beta^2)/(Q-4\alpha) + K(k)]$$

$$Br = (I*\mu_0)/(2*\Pi*R)*\gamma/(sqrQ)\ [E(k)*(1+\alpha^2+\beta^2)/(Q-4\alpha) - K(k)]$$

With

$\alpha = D_2/R$

$\beta = D_1/R$

$\gamma = D_1/D_2$

$Q = (1+\alpha)^2 + \beta^2$

K(k) and E(k) are elliptic integral functions

$\mu_0 = 4\Pi*10^{-7}$

Value of D1 and D2 for point A with regard to center of the section 25
D1 = 0.87 m
D2 = 0.684 m

Value of D1 and D2 for point F with regard to center of the section 30
D1 = 0.345 m
D2 = 0.487 m

3.4.1 Evaluation of the field generated at the switching frequency

3.4.1.1 Magnetic field of Section 25 at point A

Considering the maximum current variation is $\Delta I = 0.38$ A (see § 2.3.1) at section level.

Section 25 is constituted of 5 strings :

Section	String	Area main (m²)	Area redundant (m²)
25	37	-0.123	0.047
	38	-0.162	-0.090
	39	-0.211	-0.112
	40	-0.274	-0.130
	41	-0.312	-0.162

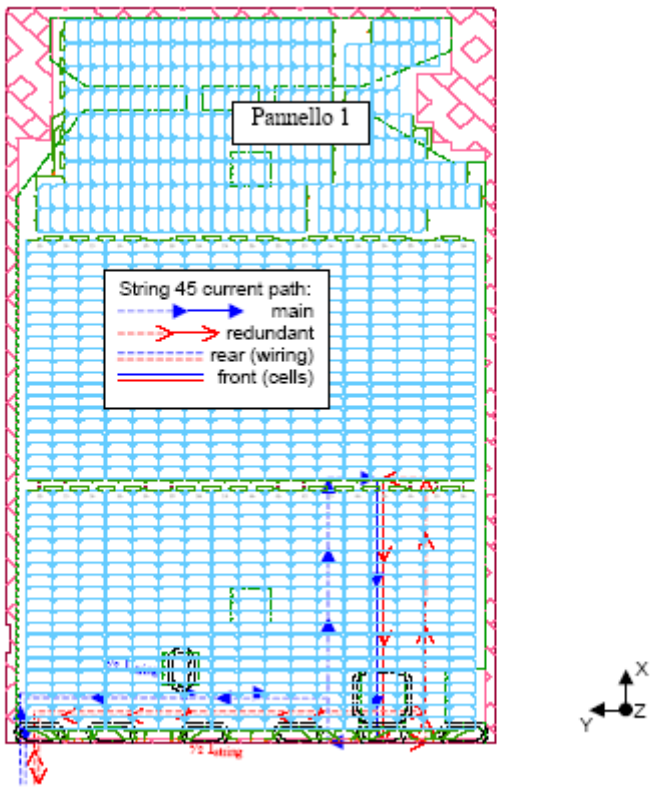

Figure 2.4.1-1 : String 45, typical current path (extracted from [RD 03])

The variation of the current at string level is 0.38/5 = 0.076A and at half string level 0.038A.

The total loop area obtained by adding the string area (main and redundant) is 1.576 m²

This area is equivalent to a loop with a radius of 0.71 m

The evaluation of the field generated by section 25 at point A level is performed taking into account the following values :

I = 0.038 A

R= 0.71m

D1 = 0.87m

D2=0.684 m

The result is Bx = 4.33 nT and Br = 4.13 nT

Field amplitude is B = 6 nT i.e. 75 dBpT

3.4.1.2 Magnetic field of section 30 at point F

Considering the maximum current variation is $\Delta I = 0.38$ A (see § 2.3.1) at section level.

Section 30 is constituted of 5 strings :

Section	String	Area main (m²)	Area redundant (m²)
30	42	-0.121	-0.038
	43	-0.082	0.120
	44	-0.054	0.143
	45	-0.008	0.226
	46	0.152	0.264

The variation of the current at string level is 0.38/5 = 0.076A and at half string level 0.038A.

The total loop area obtained by adding the string area (main and redundant) is 0.602 m²

This area is equivalent to a loop with a radius of 0.44 m.

The evaluation of the field generated by section 30 at point F level is performed taking into account the following values :

I = 0.038 A

R= 0.44m

D1 = 0.345 m

D2 = 0.487 m

The result is Bx = 7.56nT and Br = 14.2 nT

Field amplitude is B = 16 nT i.e. 84 dBpT

Nota : The magnetic field evaluation taking into account each string individually gives a similar value of B = 16.5 nT

3.4.2 Evaluation of the magnetic field generated by the transients

Simulations have been performed using the model presenteded in annex 2 and adapted with the following values
Bus voltage : 28 V
Solar array section capacitance : 500 nF
Wiring inductance : 2*2 µH

Results are presented hereafter :

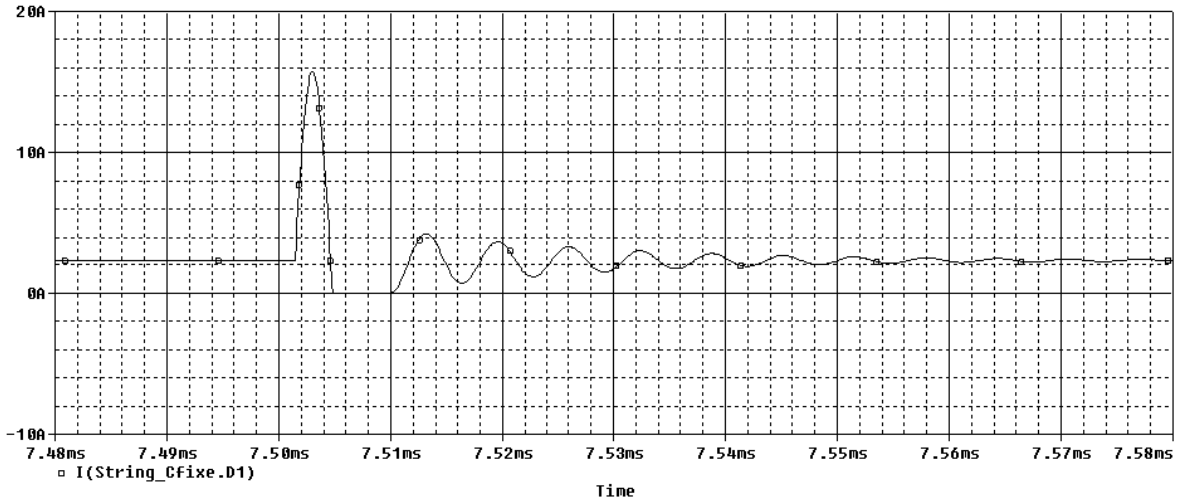

Figure 2.4-1 : Current at shunt closure at section output

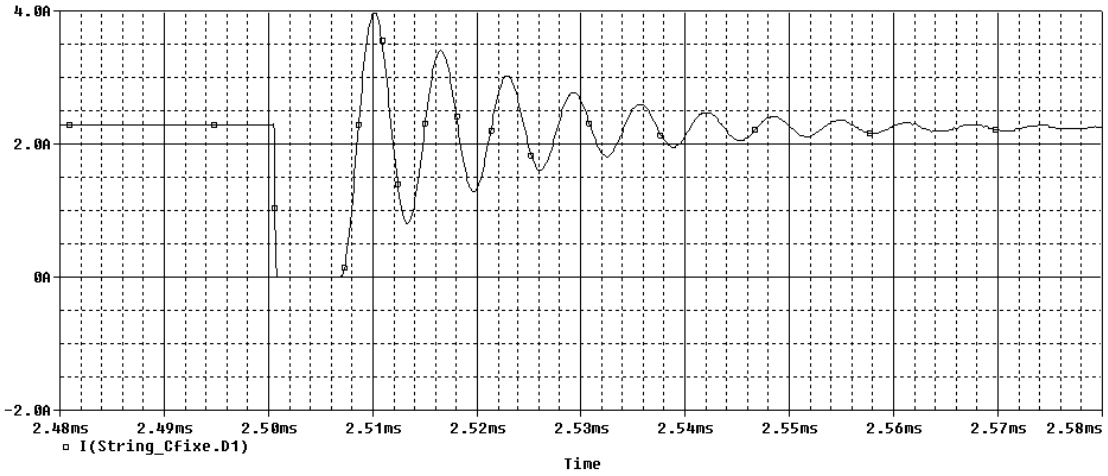

Figure 2.4-2 : Current at shunt opening at section output

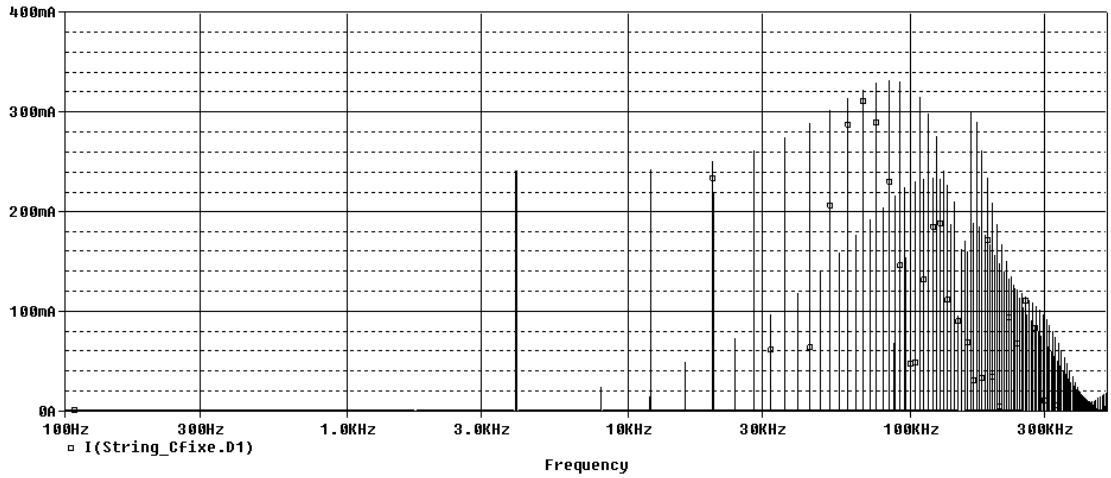

Figure 2.4-3 : Fourier transform of current at shunt opening and closure

The analysis of the results obtained at shunt closure (figure 2.4-1) shows that the values are similar to the measurements performed for the solar array section capacitance (see annex 4).

As the section contains 5 identical strings, we can consider that the transient amplitude at string level is the transient amplitude at section level divided by 5.

In fact as the solar array capacitance is distributed along the strings, the transient at string level output is the maximum value. However as the loops formed by the two current paths (main and redundant) a large part of the loop being constituted of wires, we can consider that the error will be lower than 25 % if the maximum value is taken into account.

In time domain the transient value reaches 15 A at section level, it conducts to a value of 3 A at string level, and 1.5 A at half string level.

In frequency domain the same approach can be considered, it conducts to have a maximum value of 330 mA/(2*5) = 33 mA at 90 kHz.

3.4.2.1 Magnetic field of Section 25 at point A level

The evaluation of the field generated by section 25 at point A level is performed taking into account the following values :

I = 0.033 A at 90 kHz

R= 0.71m

D1 = 0.87m

D2=0.684 m

The result is Bx = 3.75 nT and Br = 3.60 nT

Field amplitude is B = 5.2 nT i.e. 74 dBpT

3.4.2.2 Magnetic field of section 30 at point F

The evaluation of the field generated by section 30 at point F level is performed taking into account the following values :

I = 0.033A at 90 kHz

R= 0.44m

D1 = 0.345 m

D2 = 0.487 m

The result is Bx = 6.5 nT and Br = 12.4 nT

Field amplitude is B = 14 nT i.e. 83 dBpT

4. ANALYSIS

The magnetic field generated by the Herschel solar array on PACS cryo-harness have been evaluated, results are summarised in the following table :

Solar array section	Frequency	At point A level (dBpT)	At point F level (dBpT)
25	S3R switching	75	
25	90 kHz	74	
30	S3R switching		84
30	90 kHz		83

By doing a cross check with the values evaluated in the frame of other programs (see annex 3 and 5), the order of the values obtained is correct. An error lower than 10 dB can be considered.

Section 25 is one of the worst sections of the Herschel solar array, this section is not correctly compensated with regard to the magnetic moment (the value is 10 times higher as for the best compensated sections) , it explains the relative high value of the magnetic field obtained at cryo-harness level.

Considering section 30 and point F, the distance between them is low and explains the high value of the magnetic field obtained.

An other aspect which have to be considered is that PACS sensors can be sensitive in a large frequency band (e.g. some hundreds kHz). It can be of interest to perform a test with a time domain transients at the S3R switching rate .

5. CONCLUSION

The solar array is compliant with its magnetic moment requirement of 1 Am^2. However, magnetic field values of 84 dBpT can be generated by the Herschel solar array on the PACS cryo-harness.

The radiated susceptibility tests performed on Herschel EQM have shown the following susceptibility levels for PACS photometer :

90 dBpT from 30 Hz up to 20 kHz
80 dBpT from 20 kHz up to 50 kHz

This is in deviation w.r.t. the radiated susceptibility H-field requirement (EMCEQ-250 of RD04) which asks for 140 dBpT susceptibility level between 30 Hz and 50 kHz (see H-P-PACS-RFW-004).

Today considering the worst case, we have no margin between the susceptibility level and the field generated by the solar array at point F level.

The proposed approach to restore a margin is the following:

- Check of potential magnetic loops in the harness at point F level
- Check is any loops exist at SVM/H-PLM struts level due to the cryo-harness routing
- Analyse possibility to implement a magnetic shield, compliant with thermal requirements, to protect the PACS cryo harness cables.

In order to check at FM satellite level the compatibility between Solar Array and PACS, it is proposed to add to the radiated susceptibility test a time domain injection of the magnetic field at most critical points close to the cryo harness.

APPENDICES : 1

HERSCHEL Mechanical layout

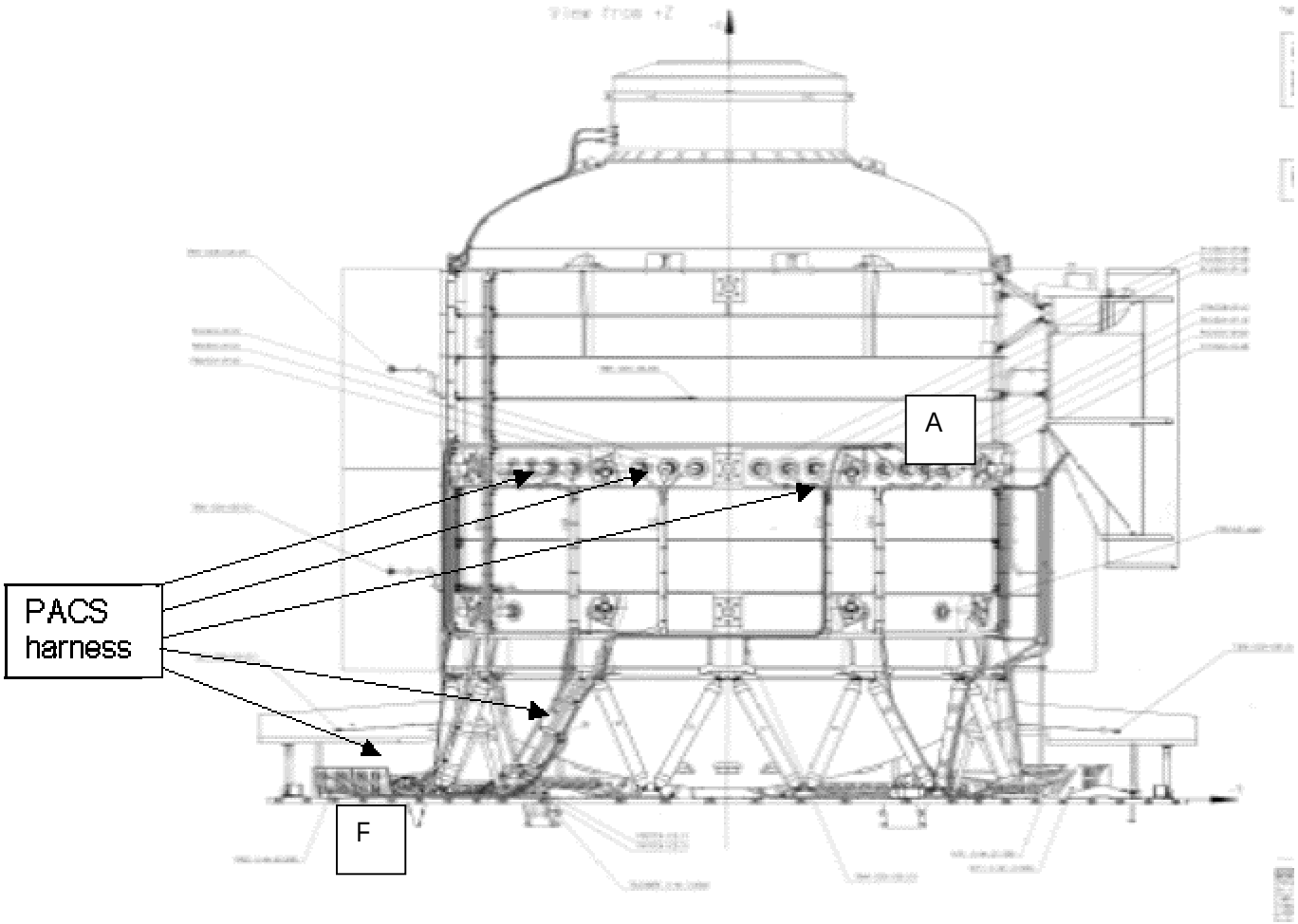

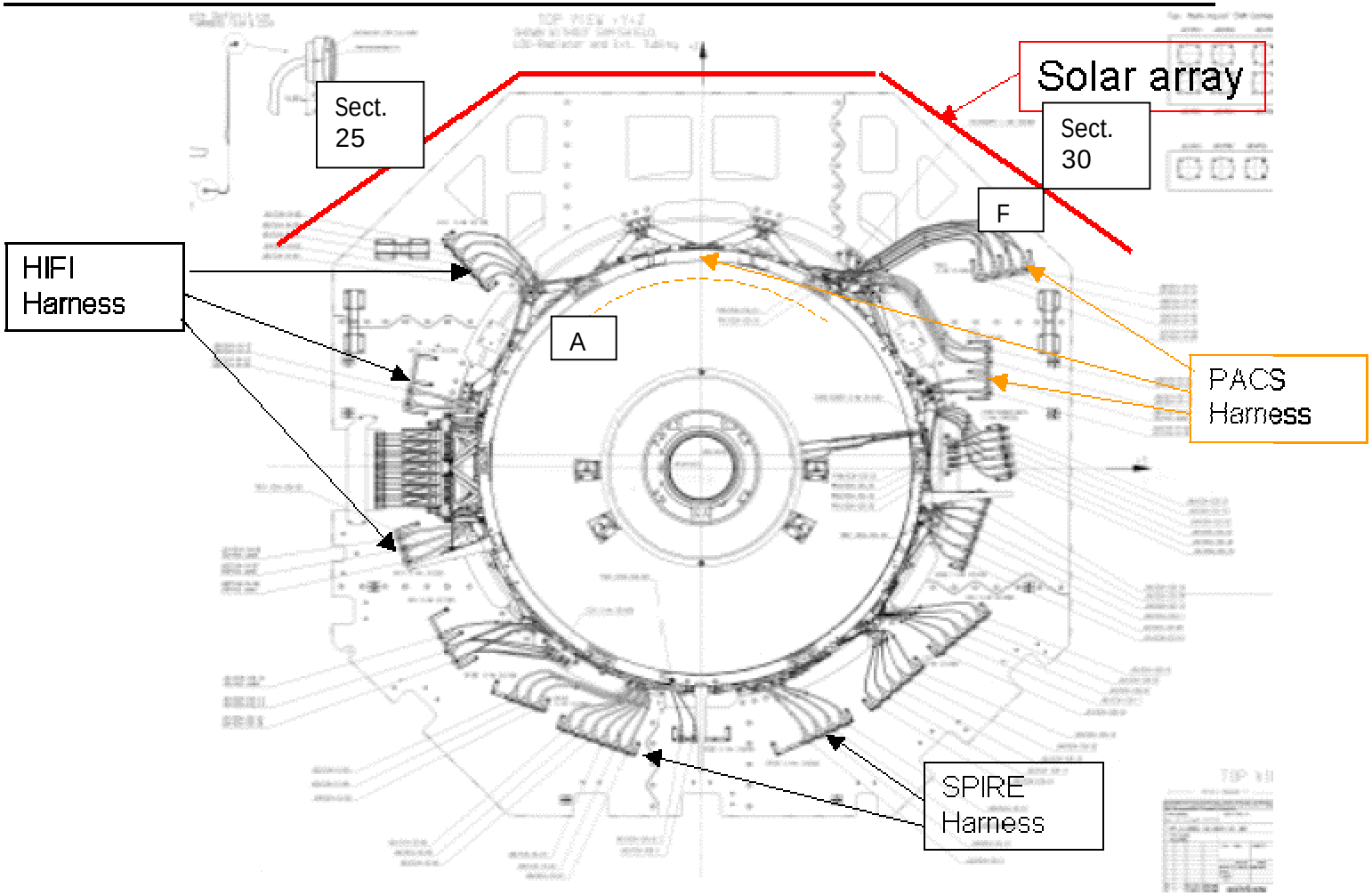

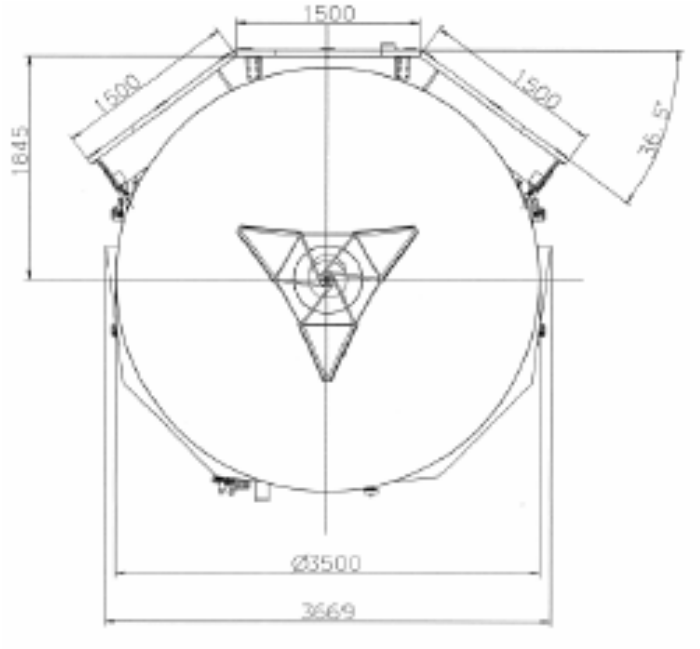

APPENDICES : 2

Measurement and simulation of the current variation in the solar array during shunt switching

Coupled tests between solar strings and a Sequential Switching Shunt Regulator

To analyse the influence of the solar array capacitance on the behaviour of the power conditioned electronics, coupled test between one string and a S3R has been realized.
The electrical scheme with a string composed of 273 non-IBF silicon Sharp 100µm/2ohm cells is displayed Figure 2.
This string under test is composed of 7 small strings ; for each string, cells are matched at 1% but the different strings are not matched; they have different grades. The panels are connected to ground via a 20kΩ resistance. A free wheel diode may be also connected in parallel with the string. A flasher illuminates the cells during several milliseconds. Several measurements are recorded on an oscilloscope (SA current, SA voltage, S3R voltage, differential voltage of each section). Different parameters (length of the harness, number of cells, lighting incidence, commutation frequency) were modified in order to analyse their influence on the transients.

A detailed PSpice model of the coupling of the solar array and the S3R has been elaborated and correlated with these tests.

One solar cell is modelled as shown on Figure 1, this model taking into account the variation of the silicon solar cells parasitic capacitance Cp with the voltage cell.

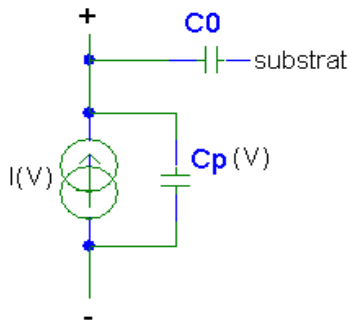

Figure 1 : Solar cell modelisation

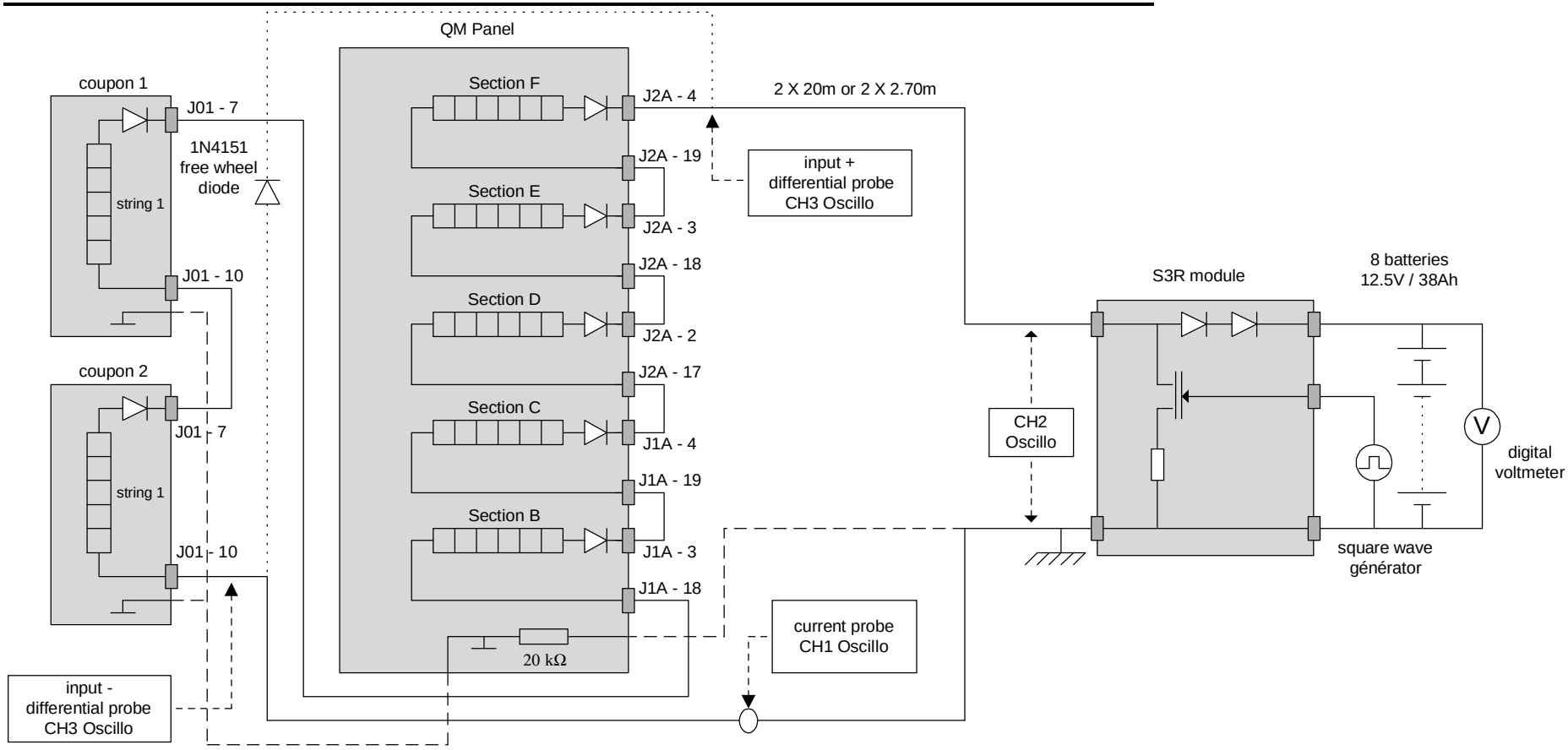

Figure 2 : Test electrical scheme

The dynamic behaviour of one string is determined by analysing the parasitic capacitance network of n solar cells in series.

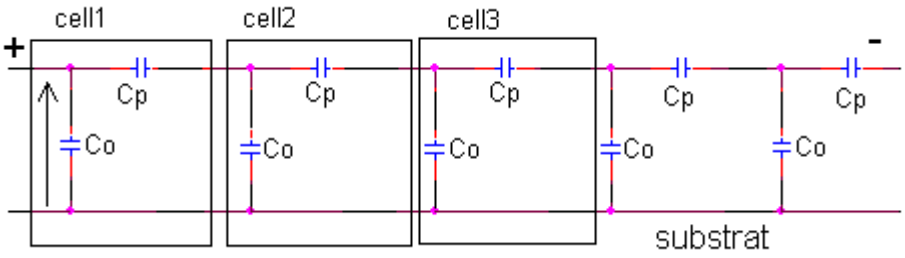

Figure 3 : String capacitive network

If all the parasitic capacitances Cp are equal, the string can be considered as a chain of n identical quadripoles.

The model of one string is thus presented Figure 4, Rcell being the cell inter-connexion resistance, the capacitances C+/-, Csub+ and Csub- of the string being a function of the capacitances values Cp and C0 and of the number of solar cells.

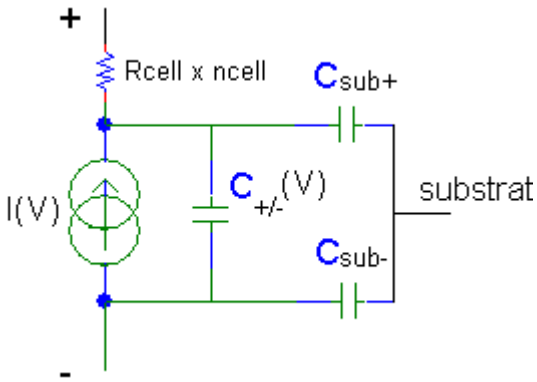

Figure 4 : Solar string modelisation

In the test Pspice model, the parameters of each small string have been adjusted in order to take into account the dis-matching between the strings. Indeed, as the strings were not perfectly matched, the voltage sharing was not uniform. Some cells were reversed polarised during shunt closure as shown on Figure 5.

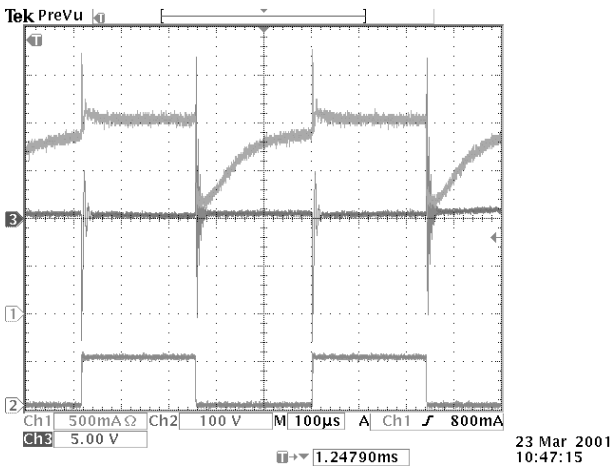

Figure 5 : Differential voltage string E

These Pspice simulations have been correlated with the experimental results as shown Figure 6 and Figure 7. This model has then been used to predict current and voltage transients due to shunt regulation for in flight configurations.

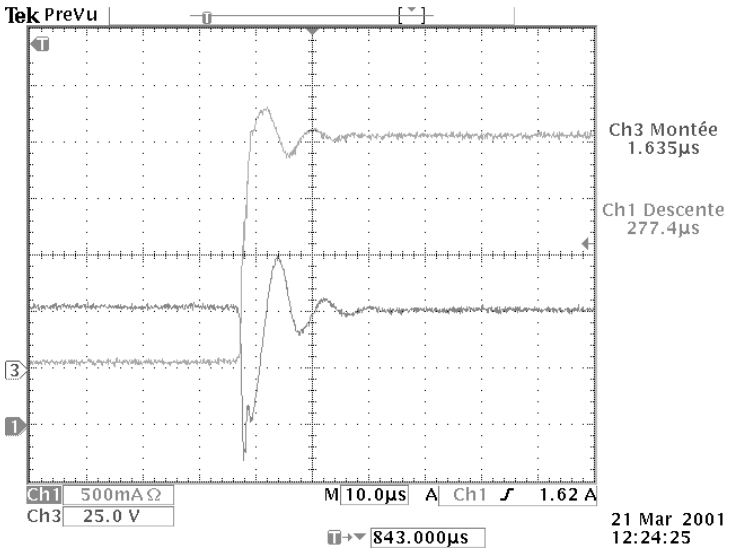

Ch1 : string current (500mA/div)
Ch3 : string voltage (25V/div)

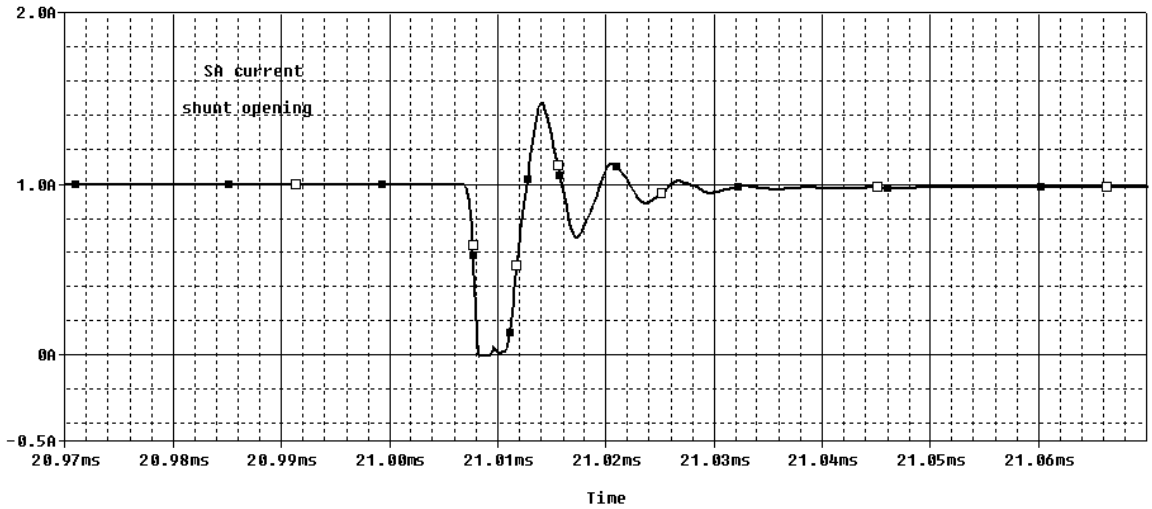

Figure 6 : Current transient at shunt opening (test and simulation)

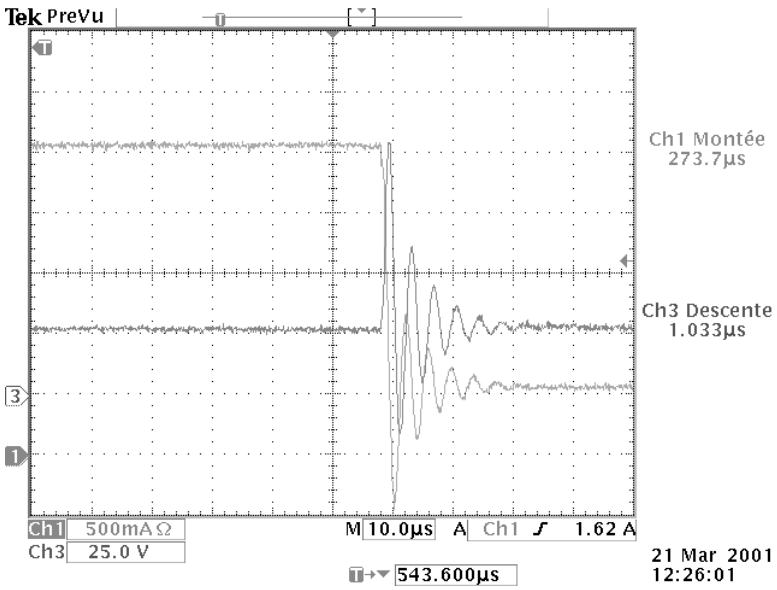

Ch1 : string current (500mA/div)
Ch3 : string voltage (25V/div)

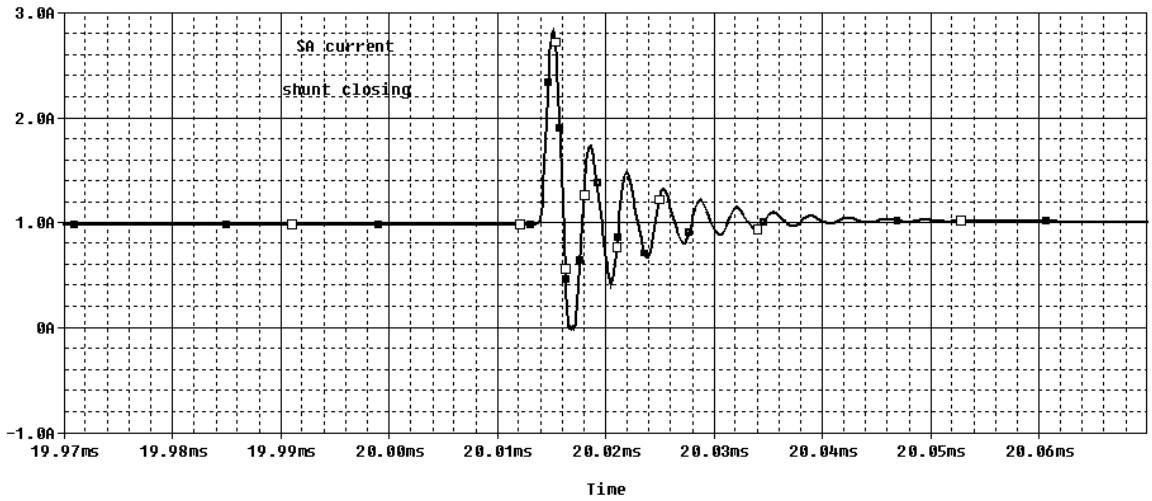

Figure 7 : Current transients at shunt closing (test and simulation)

APPENDICES : 3

Magnetic field evaluation on MSG

Main results of the evaluation of the magnetic field generated by the solar array of MSG are presented in this annex.

Table 7.2-6: Summary of Simulation Results

UNIT	FIELD STRENGTH			
	Distance from S/A	E [dBµV/m] at 14 kHz	E [dBµV/m/MHz] at 14 kHz	B [dBpT] at 4 kHz
PRU	0.49 m	63.9	111.9	39.7
PCU	0.21 m	77.6	125.6	61.0
AOCE	0.31	46.4	96.3	66.9
ACU	0.07	118.5	166.5	93.1
GERB ICU	0.12	83.3	131.3	71.6
GERB MEC	0.29	57.0	105.0	42.5
CDMU	0.53	48.8	96.8	47.2
FPCA	1.6	-58.5	-18.7	50.2
1m from S/A, 45°	1	26.0	73.9	25.2
1m from S/A, 90°	1	12.7	60.7	9.1
1m from S/A, 112.5°	1	24.8	72.8	28.9
1 m from S/A, 135°	1	32.7	80.7	34.5
1m from S/A, 157.5°	1	36.9	84.8	35.0
1 m from S/A, 180°	1	38.2	86.2	37.0

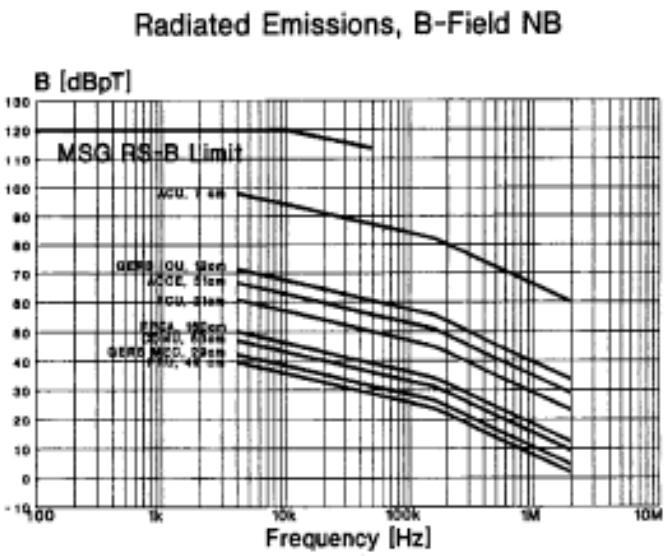

Fig. 7.2-14: Magnetic Fields at the respective Units

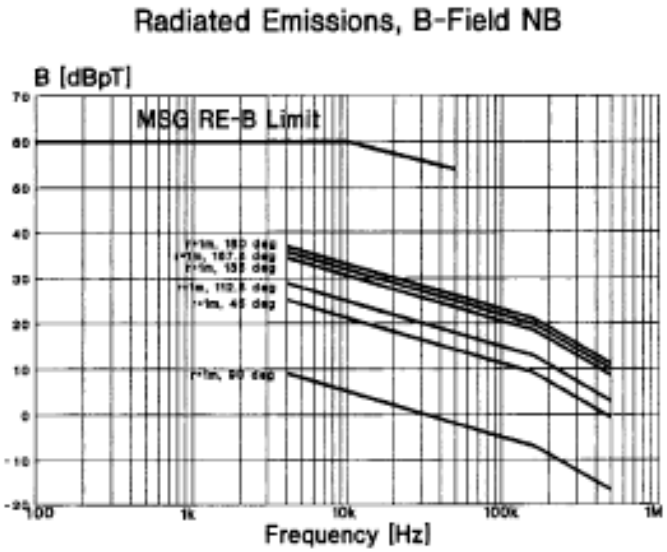

Fig. 7.2-15: Magnetic Fields at 1 m Distances

Appendices : 4

Solar Array Section Capacitance measurement on Planck

Results of the solar array section capacitance measurement performed on Planck are presented hereafter. They are extracted from [RD 02].

Capacitance / Inductance TEST

General Note :
The voltage profile cannot be represented as a simple charging of a capacitor by a constant current.
The presence of the blocking diodes (in series with the strings) cause an initial oscillation (due to the small capacitance of the diodes), being the time constant of this transient lower than the one dominated by the capacitance of the solar cell.
The results are confirmed also by the opposite transition, in which we can derive the same values of the dynamic parameters.

Item	Irradiance	String Current (Isc)	String Voltage (Voc)	rise time 20-80%	ΔV (20-80%)	Ccells
Section 10 (4 strings)	100 SC	2 A	57 V	7 µs	34 V	410 nF

Item	Series resistance (Rs)	Period of oscilattion (Trep)	Decay constant (τ)	Inductance (L)	Cblocking
Section 10 (4 strings)	≅ 1 Ω	160 ns	≅ 05 µs	250 nH	2.6 nF

Item	Irradiance	String Current (Isc)	String Voltage (Voc)	rise time 20-80%	ΔV (20-80%)	Ccells
Section 11 (5 strings)	100 SC	25 A	57 V	7 µs	34 V	410 nF

Item	Series resistance (Rs)	Period of oscilattion (Trep)	Decay constant (τ)	Inductance (L)	Cblocking
Section 11 (5 strings)	≅ 1 Ω	160 ns	≅ 05 µs	250 nH	2.6 nF

Section 10 test results :

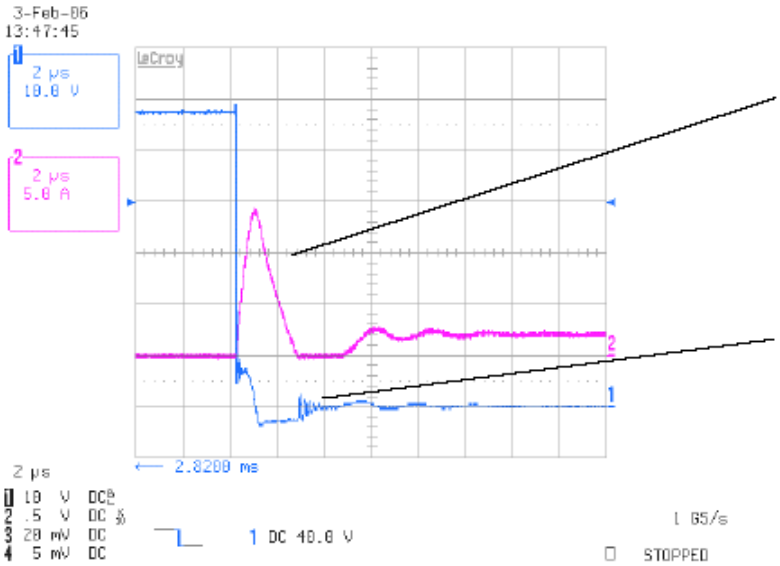

Ccell is prevalent
The valid relation is:

$$T_{REP} = 2\pi\sqrt{LC_{cell}} \quad (1)$$

Diode is blocking the negative wave
Cdiode is prevalent.
The valid relation is:

$$T_{REP} = 2\pi\sqrt{LC_{blocking}} \quad (1)$$

Section 11 test results :

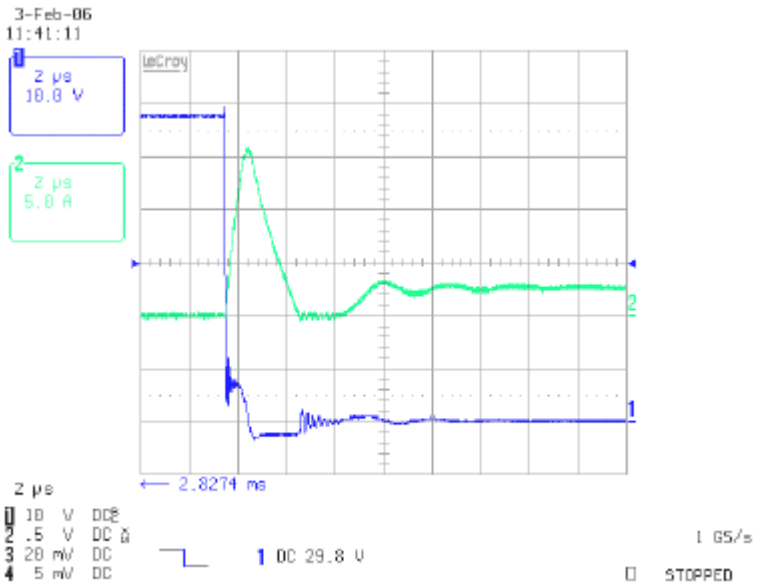

APPENDICES : 5

Results of simulations performed by a supplier in the frame of an other program

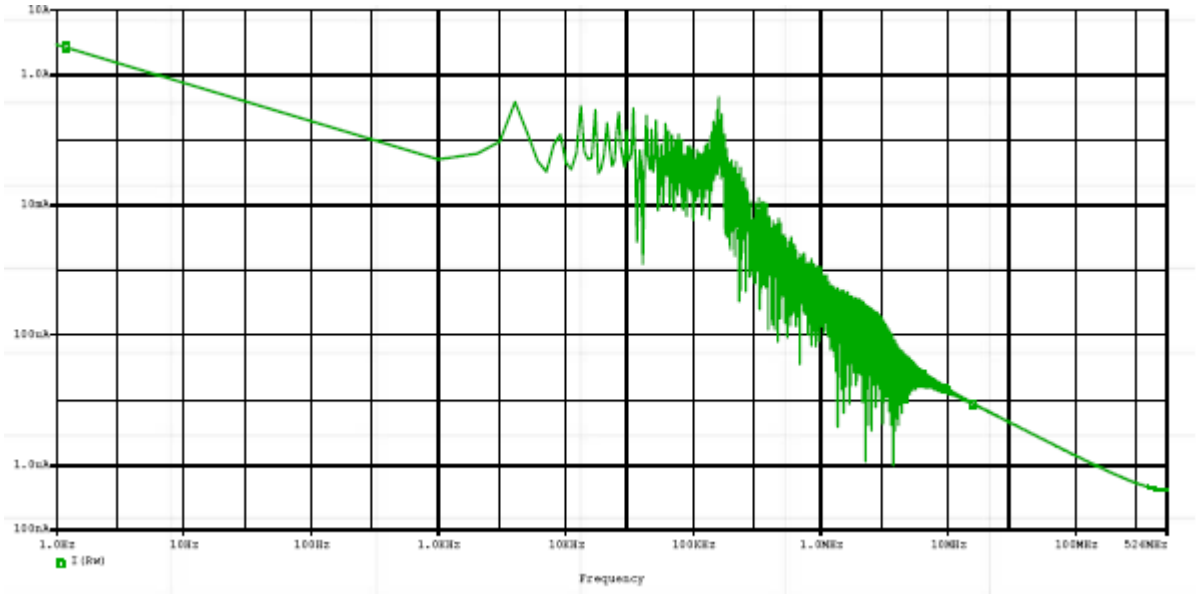

Results of an analysis performed with the following parameters :

Section current : 3 A
Harness inductance : 2µH
Section capacitance : 500 nF

END OF DOCUMENT